

Gravitational and Electromagnetic Radiations from Binary Black Holes with Electric and Magnetic Charges: I. Circular Orbits on a Poincaré Cone

Lang Liu,^{1,2,*} Øyvind Christiansen,^{3,†} Zong-Kuan Guo,^{1,2,4,‡} Rong-Gen Cai,^{1,2,4,§} and Sang Pyo Kim^{1,5,¶}

¹*CAS Key Laboratory of Theoretical Physics, Institute of Theoretical Physics,
Chinese Academy of Sciences, Beijing 100190, China*

²*School of Physical Sciences, University of Chinese Academy of Sciences, No. 19A Yuquan Road, Beijing 100049, China*

³*Institute of Theoretical Astrophysics, University of Oslo, Sem Sælands vei 13, 0371 Oslo, Norway*

⁴*School of Fundamental Physics and Mathematical Sciences, Hangzhou Institute for Advanced Study,
University of Chinese Academy of Sciences, Hangzhou 310024, China*

⁵*Department of Physics, Kunsan National University, Kunsan 54150, Korea*

(Dated: November 9, 2021)

We derive the effective one-body motion of the dyonic binary and explore features of the static orbit including the chaotic behavior. By using the post-Newtonian method, we calculate the total emission rate of energy and angular momentum due to gravitational radiation and electromagnetic radiation for circular orbits on a Poincaré Cone. Moreover, we get the evolution of the orbit and calculate the merger time of the dyonic binary. We find the electric and magnetic charges could significantly suppress the merger time of the dyonic binary. The results of this paper provide rich information on the dyonic binary and can be used to test black holes with magnetic charges.

I. INTRODUCTION

The first direct detection of gravitational waves (GWs) from a binary black hole coalescence [1] has opened a new window of physics and astronomy. Ten merger events of binary black holes have been reported by LIGO/Virgo during the O1 and O2 observing runs over the past few years [1–7]. The progenitors of these binaries are under intensive investigation and still unknown [8–12]. These LIGO/Virgo black holes show a much heavier mass distribution than the mass distribution inferred from X-ray observations [13–15], which would present a gigantic challenge to the formation and evolution mechanisms of astrophysical black holes. One possible explanation for LIGO/Virgo black holes is the primordial black holes (PBHs) [8, 9, 11, 16–19] formed in the radiation-dominated era of the early universe due to the collapse of large energy density fluctuations [20, 21]. Beside being the sources of LIGO/Virgo detection, PBHs can also be a candidate of dark matter or the seeds for galaxy formation [22–24].

Dirac introduced magnetic monopoles to explain the quantization of charges and to make the Maxwell equations symmetric under the duality of electric and magnetic fields. Schwinger studied quantum field theory for particles with electric and magnetic charges, the so-called dyons [25]. The Einstein-Maxwell theory has spherically symmetric black holes with electric and magnetic charges and rotating dyonic black holes [26]. Magnetic black holes could be regular in a nonlinear electrodynamics theory [27].

The standard model of particle physics predicts 't Hooft-Polyakov monopoles from Yang-Mills theory (for review and references, see Ref. [28]). Though no evidence of magnetic monopoles has been found yet at laboratories [29, 30], primordial magnetic monopoles would have been produced [31] and formed magnetically charged black holes [32, 33] if the standard model is the correct theory in the early universe. Recently, the electroweak phase transition has been studied in magnetic black holes [34].

Black holes can have additional hairs of electric and magnetic charges as well as the mass and angular momentum. This provides charged black holes with a rich structure than those without charges. The binary of charged black holes with electric charges emits not only GWs but also electromagnetic waves. In the Post-Newtonian method for a binary of charged black holes, the Coulomb force gives an additional central force to the gravitational force and thus modifies the Keplerian orbit by the relative ratio of the Coulomb force to the gravitational force [35]. This ratio affects the power distribution of GWs and leads to a different power-law of the merger rate.

In this paper we investigate the binary of black holes with electric and magnetic charges in the Einstein-Maxwell theory. The nonrotating black hole with an electric charge q and a magnetic charge g , the so-called dyonic black hole, has the same metric as the Reissner-Nordström black hole with q^2 replaced by $q^2 + g^2$, and the rotating dyonic black hole has a similar structure [26]. In the post-Newtonian method, the magnetic charge of dyonic black hole gives rise to an angular momentum-dependent, noncentral force to the central force of the electric and gravitational forces, and drastically changes the orbit of a binary of black holes with electric and magnetic charges. The extremal dyonic black holes can remain stable against the Hawking radiation and Schwinger emission of electric charges [36] provided that the magnetic charges dominate the electric charges and suppress

* liulang@itp.ac.cn

† oyvind.christiansen@astro.uio.no

‡ guozk@itp.ac.cn

§ cairg@itp.ac.cn

¶ sangkim@kunsan.ac.kr

the Schwinger effect and the monopole production.

A binary of dyonic black holes has a generalized angular momentum, which is a conserved Laplace-Runge-Lenz vector, around which the orbital plane precesses and which confines the orbits to a Poincaré cone [37]. On the Poincaré cone, the binary follows the Keplerian orbits with the conserved energy and angular momentum squared modified by the magnetic charges. The emission power of electromagnetic waves and GWs thus drastically changes, which may provide a new window to identify the primordial magnetic charges.

In this paper, we will derive the effective one-body motion of the dyonic binary and investigate characteristics of the static orbits. The total emission rate of energy and angular momentum due to gravitational radiation and electromagnetic radiation is calculated within the post-Newtonian method for circular orbits on a Poincaré Cone (the case of $e = 0$). Moreover, we get the evolution of the orbit and calculate the merger time of the dyonic binary. We find the electric and magnetic charges could significantly suppress the merger time of the dyonic binary. The rest of this paper is organized as follows. In the next section, we derive the effective one-body motion of the dyonic binary. In Sec. III, we explore features of the static orbits including the chaotic behavior. In Sec. IV, we calculate the total emission rate of angular momentum and energy due to gravitational radiation and electromagnetic radiation, derive the evolution of a and θ and find the merger time. The final section is devoted to conclusion.

II. EQUATION OF ORBIT

In the post-Newtonian method we study the orbital motion of a binary of black holes with electric and magnetic charges. Maxwell's equations with magnetic monopoles are given by¹:

$$\begin{cases} \nabla \cdot \mathbf{E} = 4\pi\rho_e, \\ \nabla \times \mathbf{E} = -4\pi\mathbf{j}_m - \partial\mathbf{B}/\partial t, \\ \nabla \cdot \mathbf{B} = 4\pi\rho_m, \\ \nabla \times \mathbf{B} = 4\pi\mathbf{j}_e + \partial\mathbf{E}/\partial t, \end{cases} \quad (1)$$

where ρ_m is a magnetic charge density and \mathbf{j}_m is a magnetic current. The Lorentz force on a dyon with an electric charge q and a magnetic charge g is

$$\mathbf{F} = q(\mathbf{E} + \mathbf{v} \times \mathbf{B}) + g(\mathbf{B} - \mathbf{v} \times \mathbf{E}). \quad (2)$$

The point dyon generates the electric and magnetic fields

$$\mathbf{E} = q\frac{\mathbf{r}}{r^3}, \quad \mathbf{B} = g\frac{\mathbf{r}}{r^3}. \quad (3)$$

In this paper we consider a black hole binary with electric and magnetic charges (q_1, g_1) and (q_2, g_2) , that is,

nonrotating dyonic black holes with the metric

$$ds^2 = -f(r)dt^2 + \frac{dr^2}{f(r)} + r^2 d\Omega_2^2, \quad (4)$$

where

$$f(r) = 1 - \frac{2m_i}{r} + \frac{q_i^2 + g_i^2}{r^2}, \quad (i = 1, 2). \quad (5)$$

The nonrelativistic interaction of two dyons was studied in classical theory in Ref. [38] and in a quantum theory [39]. We will study the bounded motion of two dyonic black holes as a binary system. The Keplerian motions with or without a force term of angular momentum are classified [37].

For a binary of dyonic black holes, we choose the center of mass system at the origin

$$r_1^i = -\frac{m_2}{M}R^i, \quad r_2^i = \frac{m_1}{M}R^i, \quad (6)$$

where

$$R^i = r_2^i - r_1^i, \quad M = m_1 + m_2. \quad (7)$$

Considering the Lorentz force and gravitational force, the equation of motion is given by

$$m_2\ddot{r}_2^i = \mu\ddot{R}^i = C\frac{R^i}{R^3} - D\epsilon_{jk}^i\frac{R^j}{R^3}v^k, \quad (8)$$

where

$$\mu = \frac{m_1m_2}{M}, \quad v^i = \dot{R}^i, \quad (9)$$

$$C = (-\mu M + q_1q_2 + g_1g_2), \quad D = (q_2g_1 - g_2q_1). \quad (10)$$

Note that $D = 0$, which corresponds to purely electric or magnetic charges or $q_2/q_1 = g_2/g_1$ of balancing out the velocity-dependent Lorentz forces, yields the same orbital motion as purely electric charges. Here, we rewrite Eq. (8) as

$$\mu\ddot{\mathbf{R}} = C\frac{\mathbf{R}}{R^3} - D\frac{\mathbf{R}}{R^3} \times \mathbf{v}, \quad (11)$$

and cross the left hand side with \mathbf{R} . Then we get

$$\mu\epsilon_{jk}^i R^j \ddot{R}^k = \frac{d}{dt} \left(\mu\epsilon_{jk}^i R^j \dot{R}^k \right) = \frac{d}{dt} \tilde{L}^i, \quad (12)$$

where $\tilde{\mathbf{L}} \equiv \mu\mathbf{R} \times \mathbf{v}$ is the real angular momentum of the binary system. Writing the right hand side as

$$\begin{aligned} \dot{\tilde{L}}^i &= -D\epsilon^{ijk}R_j\epsilon_{klm}\frac{R^l}{R^3}\dot{R}^m \\ &= -\frac{D}{R^3} \left(\delta_l^i\delta_m^j - \delta_m^i\delta_l^j \right) R_j R^l \dot{R}^m \\ &= \frac{D}{R} \left(\dot{R}^i - R^i \dot{R}/R \right), \end{aligned} \quad (13)$$

and using the relation

$$\dot{\hat{r}} = \frac{d}{dt} \left(\frac{R^i}{R} \right) \hat{\mathbf{x}}_i = \frac{1}{R} \left(\dot{R}^i - R^i \dot{R}/R \right) \hat{\mathbf{x}}_i, \quad (14)$$

¹ In this paper, we choose units of $G = c = 4\pi\epsilon_0 = \frac{\mu_0}{4\pi} = 1$.

where $\hat{\mathbf{r}}$ is the unit vector along \mathbf{R} and $\hat{\mathbf{x}}_i$ is the unit vector along x_i axis, we find a conserved quantity

$$\dot{\mathbf{L}} = 0, \quad \mathbf{L} \equiv \tilde{\mathbf{L}} - D\hat{\mathbf{r}}. \quad (15)$$

Note that \mathbf{L} is a Laplace-Runge-Lenz vector [37] and has a meaning of the generalized angular momentum of the binary system. From the definition (15) and the fact that $\tilde{\mathbf{L}}$ is perpendicular to $\hat{\mathbf{r}}$, we can obtain

$$(L)^2 = (\tilde{L})^2 + D^2. \quad (16)$$

Since \mathbf{L} is conserved and D is a constant, we arrive at the fact that the magnitude of the real angular momentum \tilde{L} is conserved even though the direction of $\tilde{\mathbf{L}}$ changes. Notice that the definitions of \mathbf{L} and $\tilde{\mathbf{L}}$ lead to the result

$$\mathbf{L} \cdot \hat{\mathbf{r}} = (\mu\mathbf{R} \times \mathbf{v} - D\hat{\mathbf{r}}) \cdot \hat{\mathbf{r}} = -D, \quad (17)$$

where we have used the fact that $\mathbf{R} \times \mathbf{v} \cdot \hat{\mathbf{r}} = 0$. By interpreting $\mathbf{L} \cdot \hat{\mathbf{r}}$ as the projection of $\hat{\mathbf{r}}$, we define the angle Ω for a Poincaré cone as

$$\cos \Omega = \frac{\mathbf{L} \cdot \hat{\mathbf{r}}}{L}, \quad (18)$$

which, as seen from Eq. (17), is constant, with a value

$$\Omega = \arccos\left(-\frac{D}{L}\right). \quad (19)$$

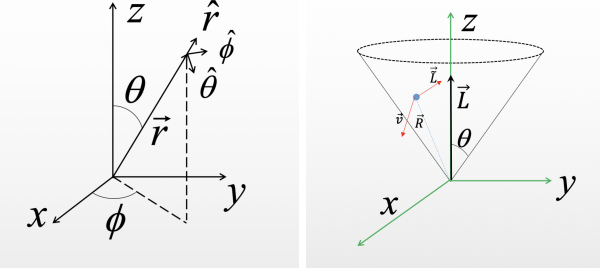


FIG. 1. [Left panel] Choice of naming convention for spherical coordinates. [Right panel] Schematic illustration on the Poincaré cone.

Now, we derive the equation of the orbits. To proceed further, we may do a trick. Because \mathbf{L} is conserved, we can pick our coordinate system to have it point along the z -axis: choose \mathbf{L} coincides with the polar axis. Using $\hat{\mathbf{z}} = \hat{\mathbf{r}} \cos \theta - \hat{\boldsymbol{\theta}} \sin \theta$, in spherical coordinates (r, ϕ, θ) , we have

$$\mathbf{L} = L\hat{\mathbf{z}} = L \begin{pmatrix} \cos \theta \\ 0 \\ -\sin \theta \end{pmatrix} = \tilde{\mathbf{L}} - D\hat{\mathbf{r}} = \begin{pmatrix} 0 \\ \tilde{L}_\phi \\ \tilde{L}_\theta \end{pmatrix} - D \begin{pmatrix} 1 \\ 0 \\ 0 \end{pmatrix}, \quad (20)$$

which means

$$\cos \theta = -D/L = \cos \Omega, \quad (21)$$

and

$$\theta = \Omega. \quad (22)$$

The special case of $D = 0$ gives an orbit on the equatorial plane. Thus, the orbit equation is given by

$$\mathbf{R} = R \begin{pmatrix} \sin \theta \cos \phi \\ \sin \theta \sin \phi \\ \cos \theta \end{pmatrix}. \quad (23)$$

For the energy, we have

$$\begin{aligned} E &= \frac{1}{2}\mu v^2 + \frac{C}{R} = \frac{1}{2}\mu(v_{\parallel}^2 + v_{\perp}^2) + \frac{C}{R} \\ &= \frac{1}{2}\mu\dot{R}^2 + \frac{\tilde{L}^2}{2\mu R^2} + \frac{C}{R}, \end{aligned} \quad (24)$$

where $v_{\parallel} \equiv \dot{R}\hat{\mathbf{r}}$ is the velocity along \mathbf{R} and

$$\mathbf{v}_{\perp} \equiv R\dot{\phi}\sin\theta\hat{\boldsymbol{\phi}} + R\dot{\theta}\hat{\boldsymbol{\theta}} = R\dot{\phi}\sin\theta\hat{\boldsymbol{\phi}} \quad (25)$$

is the velocity which is perpendicular to \mathbf{R} . To start with, we can solve Eq. (24) for \dot{R} and obtain

$$\dot{R} = \sqrt{\frac{2}{\mu}} \sqrt{E - \frac{\tilde{L}^2}{2\mu R^2} - \frac{C}{R}}. \quad (26)$$

From the definition, the conserved module of the real angular momentum can be expressed by

$$\tilde{L} \equiv \mu|\mathbf{R} \times \mathbf{v}| = \mu R v_{\perp} = \mu R^2 \sin \theta \dot{\phi}, \quad (27)$$

while the conserved module of the generalized angular momentum is given by

$$L = \frac{\tilde{L}}{\sin \theta} = \mu R^2 \dot{\phi}. \quad (28)$$

For the equation of the orbit, we need the relationship of R and ϕ by eliminating the parameter t . By using the substitution of Eqs. (26) and (28), we get

$$\frac{\dot{\phi}}{\dot{R}} = \frac{d\phi}{dR} = \left(\frac{2\mu E}{L^2} R^4 - \frac{2\mu C}{L^2} R^3 - \sin^2 \theta R^2 \right)^{-\frac{1}{2}}. \quad (29)$$

Setting $x = 1/R$ and integrating by quadrature, we finally obtain the Keplerian orbit on the Poincaré cone (22)

$$\begin{aligned} R &= \frac{\frac{\tilde{L}^2}{\mu|C|}}{1 + \sqrt{1 + \frac{2\tilde{L}^2}{\mu C^2} E \cos(\phi \sin \theta)}} \\ &\equiv \frac{a(1 - e^2)}{1 + e \cos(\phi \sin \theta)}, \end{aligned} \quad (30)$$

while the conserved energy and the magnitude of angular momentum

$$E = \frac{C}{2a}, \quad (31)$$

$$\tilde{L}^2 = \mu|C|a(1 - e^2). \quad (32)$$

Note that we have recognized the equational form for the radius of a conic section and replaced the quantities in the denominator and numerator by the conic section parameters (a, e) so that we can express it in the standard Keplerian form. For the bounded motion of our binary system, $E < 0$, which means $C < 0$. From Eqs. (27) and (32), we obtain the rate of the azimuthal angle

$$\dot{\phi} = \frac{(-C)^{\frac{1}{2}} \csc(\theta) (e \cos(\phi \sin(\theta)) + 1)^2}{a^{\frac{3}{2}} (1 - e^2)^{\frac{3}{2}} \mu^{\frac{1}{2}}}. \quad (33)$$

Further, by choosing z -axis along \mathbf{L} , the orbit is explicitly given by

$$\mathbf{R} = \frac{a(1 - e^2)}{1 + e \cos(\phi \sin \theta)} \begin{pmatrix} \sin \theta \cos \phi \\ \sin \theta \sin \phi \\ \cos \theta \end{pmatrix}. \quad (34)$$

Noting that $\theta = \Omega$ is a constant, we are able to interpret Eq. (34) as a conic-shaped orbit of the black hole which is confined to the surface of the Poincaré cone, as shown in Fig. 2. In Fig. 2, we plot the orbit by choosing $a = 1, \theta = \pi/2 \times 0.6$ and $e = 0.5$. We will explore features of the orbit in the next section.

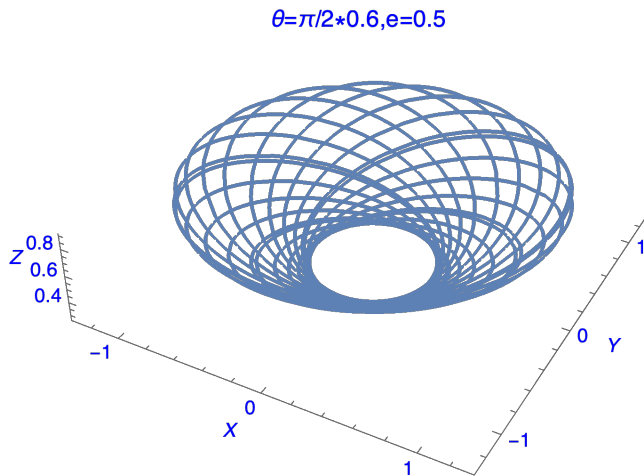


FIG. 2. A conic-shaped orbit of the black hole which is confined to the surface of the Poincaré cone by choosing ϕ from 0 to $40\pi/\sin\theta$, $a = 1, e = 0.5, \theta = \pi/2 \times 0.6$ while $\sin(3\pi/10) = (1 + \sqrt{5})/4$, according to (34). Though the orbit is bounded, it is not closed and has an infinite period in three dimensions since $\sin(3\pi/10) = (1 + \sqrt{5})/4$ is an irrational number.

III. BINARY AS A CONSERVED AUTONOMOUS SYSTEM

First, let us consider the case $e = 0$ for our binary system. From Eqs. (33) and (34), the three-dimensional

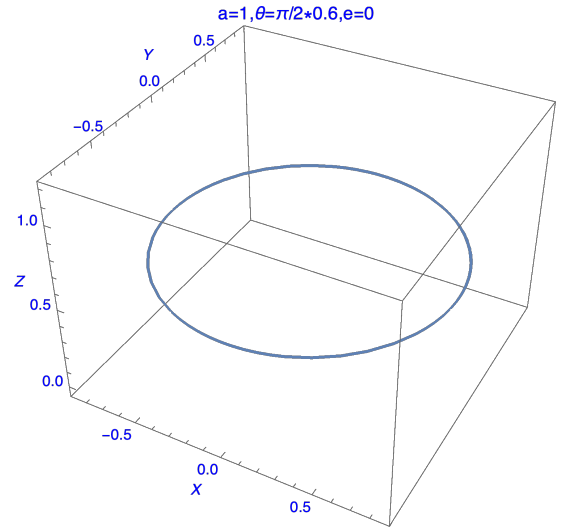


FIG. 3. A circle-shaped orbit of the black hole which is confined to the surface of the Poincaré cone by choosing $a = 1, \theta = \pi/2 \times 0.6, e = 0$, according to Eq. (35). Though $\sin(3\pi/10) = (1 + \sqrt{5})/4$ is an irrational number, the orbit is closed and has a Keplerian form while it has a finite period in three dimensions.

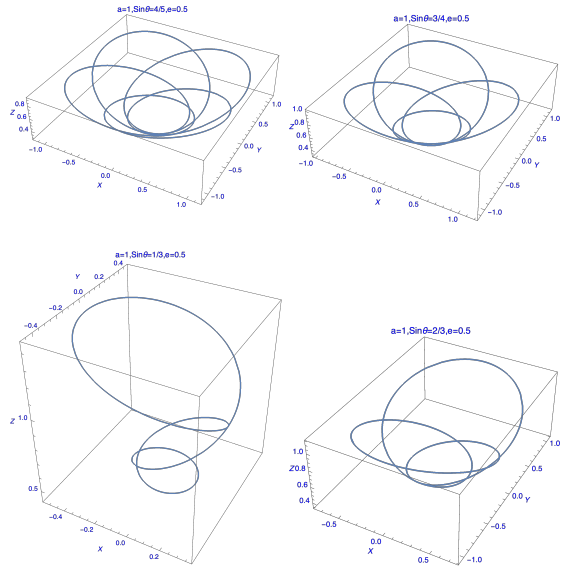


FIG. 4. Different orbits of the black hole with different θ by choosing $a = 1, e = 0.5$: $\sin \theta = 4/5$ (top left), $\sin \theta = 3/4$ (top right), $\sin \theta = 1/3$ (bottom left) and $\sin \theta = 2/3$ (bottom left).

trajectory

$$\mathbf{R} = a \begin{pmatrix} \sin \theta \cos \phi \\ \sin \theta \sin \phi \\ \cos \theta \end{pmatrix}, \quad (35)$$

is effectively a two-dimensional circular orbit with $z = \cos \theta$, and the orbital rate

$$\dot{\phi} = \frac{(-C)^{\frac{1}{2}}}{\mu^{\frac{1}{2}} a^{\frac{3}{2}} \sin \theta}, \quad (36)$$

has a finite period

$$T_1 = \int_0^{2\pi} d\phi \dot{\phi}^{-1} = 2\pi a^{3/2} \sqrt{-\mu/C} \sin \theta, \quad (37)$$

as illustrated in Fig. 3.

Next, we consider a conical elliptical orbit of $e \neq 0$ for our binary system. To get a closed orbit, we need to analyze Eq. (34). If and only if $\sin \theta$ is rational

$$\sin \theta = \frac{l}{n} \quad (38)$$

with l and n relatively positive prime numbers and $l < n$, the orbit will be closed after n revolutions, have completed exactly one ellipse and return to the initial position. In such a case, one period is given by

$$T_2 = \int_0^{2n\pi} d\phi \dot{\phi}^{-1} = 2\pi a^{3/2} \sqrt{-\mu/Cl}. \quad (39)$$

Moreover, the different numbers l and n will determine the different topology of the orbit, as shown in Fig. 4.

For $e \neq 0$, no matter how rational or irrational $\sin \theta$ is, R is a periodic function of $\phi(t)$ with the period

$$T_3 = \int_0^{2\pi/\sin(\theta)} d\phi \dot{\phi}^{-1} = 2\pi a^{3/2} \sqrt{-\mu/C}, \quad (40)$$

as shown in Fig. 5. When $e \neq 0$ and $\sin \theta$ is irrational, the orbit is not closed and shows a chaotic behavior of a conserved autonomous system [40]. In Fig. 2, we plot the orbit of the black hole by choosing $a = 1$, $\theta = \pi/2 \times 0.6$ and $e = 0.5$.

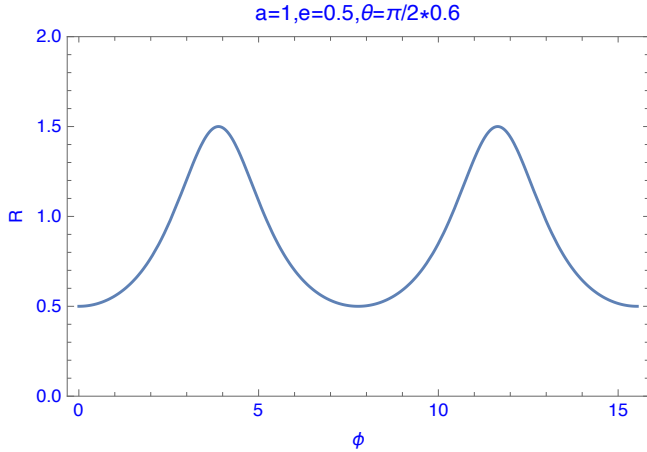


FIG. 5. The plot of R as a function of ϕ by choosing $a = 1$, $\theta = \pi/2 \times 0.6$ and $e = 0.5$, according to (34).

Now, we will explore chaotic motions of orbits by observing how two neighboring orbits deviate from each

other during their evolutions. For this, we choose two neighboring orbits $\mathbf{R}(\phi)$ and $\mathbf{R}_1(\phi)$. At time $t = 0$ (here, we choose $\phi = 0$), we set

$$\mathbf{R}_1(0) - \mathbf{R}(0) = (dx, dy, dz). \quad (41)$$

Notice that we just change the initial positions but the generalized angular momentum and the charges or C and D are fixed. Here we introduce a new parameter dl which corresponds to the distance of two Poincaré cones as shown in Fig. 6. The orbit of $\mathbf{R}_1(\phi)$ can be expressed as

$$\mathbf{R}_1 = \frac{a_1 (1 - e_1^2)}{1 + e_1 \cos((\phi + d\phi) \sin \theta)} \begin{pmatrix} \sin \theta \cos(\phi + d\phi) \\ \sin \theta \sin(\phi + d\phi) \\ \cos \theta \end{pmatrix} - dl \begin{pmatrix} 0 \\ 0 \\ 1 \end{pmatrix}, \quad (42)$$

where

$$a_1 = a + da, \quad e_1 = e + de. \quad (43)$$

From the conserved magnitude of the real angular momentum,

$$\tilde{L}^2 = \mu|C|a(1 - e^2) = \mu|C|a_1(1 - e_1^2), \quad (44)$$

we get

$$de = \frac{(1 - e^2)da}{2ae}. \quad (45)$$

To proceed further, we solve the vector equation

$$\frac{\partial \mathbf{R}}{\partial \phi} \Big|_{\phi=0} d\phi + \frac{\partial \mathbf{R}}{\partial a} \Big|_{\phi=0} da + \frac{\partial \mathbf{R}}{\partial e} \Big|_{\phi=0} de - dl \begin{pmatrix} 0 \\ 0 \\ 1 \end{pmatrix} = \begin{pmatrix} dx \\ dy \\ dz \end{pmatrix}. \quad (46)$$

Solving Eq. (46), we have

$$da = -\frac{2e \csc(\theta)}{(1 - e)^2} dx, \quad (47)$$

$$d\phi = \frac{\csc(\theta)}{a(1 - e)} dy, \quad (48)$$

$$dl = dx \cot(\theta) - dz. \quad (49)$$

Now, we introduce a new function $\lambda(\phi)$ defined as

$$\lambda(\phi) \equiv \frac{(\mathbf{R}_1(\phi) - \mathbf{R}(\phi))^2}{(\mathbf{R}_1(0) - \mathbf{R}(0))^2}, \quad (50)$$

which describes the ratio of the evolution of the distance between two neighboring orbits $\mathbf{R}(\phi)$ and $\mathbf{R}_1(\phi)$.

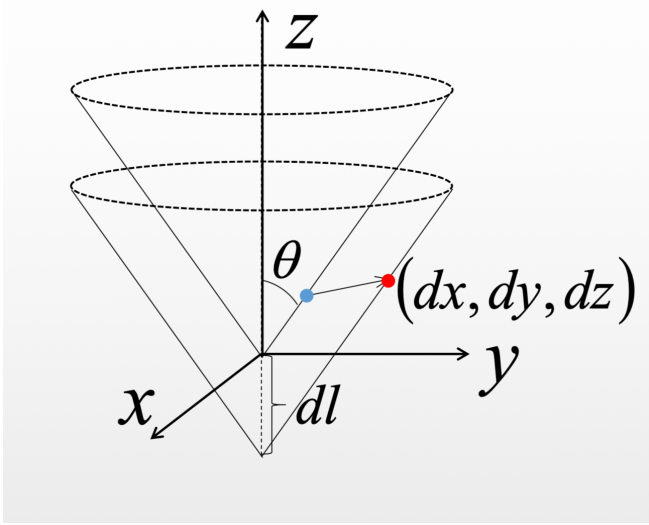


FIG. 6. Schematic illustration on two neighboring orbits $\mathbf{R}(\phi)$ and $\mathbf{R}_1(\phi)$.

For the case, $dx \neq 0$, we can set

$$\mathbf{R}_1(0) - \mathbf{R}(0) = (dx, dy, dz) = (1, k_y, k_z) \frac{dr}{\sqrt{1 + k_y^2 + k_z^2}}. \quad (51)$$

Using Eq. (42) and the definition (50), we obtain

$$\begin{aligned} \lambda(\phi) &= (k_y^2 + k_z^2 + 1)^{-1} (e \cos(\phi \sin(\theta)) + 1)^{-4} \\ &\times ((e + 1)^2 (k_y \cos(\phi)) (e \cos(\phi \sin(\theta)) + 1) \\ &+ \sin(\phi) ((e + 1) \cos(\phi \sin(\theta)) + e k_y \sin(\theta) \sin(\phi \sin(\theta))))^2 \\ &+ (e + 1)^2 (k_y \sin(\phi)) (e \cos(\phi \sin(\theta)) + 1) \\ &- \cos(\phi) ((e + 1) \cos(\phi \sin(\theta)) + e k_y \sin(\theta) \sin(\phi \sin(\theta))))^2 \\ &+ ((e + 1) \cot(\theta) ((e + 1) \cos(\phi \sin(\theta)) \\ &+ e k_y \sin(\theta) \sin(\phi \sin(\theta))) \\ &+ (k_z - \cot(\theta)) (e \cos(\phi \sin(\theta)) + 1)^2)^2, \end{aligned} \quad (52)$$

which is independent of a . $\lambda(\phi)$ is a periodic function with the same period T_3 as R , as shown in Fig. 7. The ratio of the distance to the initial one decreases and increases periodically for some ranges of ϕ . For $dl \neq 0$, or $k_z \neq 0$, two orbits $\mathbf{R}(\phi)$ and $\mathbf{R}_1(\phi)$ are confined to different Poincaré cones. When $dl = 0$ which corresponds to two orbits $\mathbf{R}(\phi)$ and $\mathbf{R}_1(\phi)$ confined to the same Poincaré cone, $\lambda(\phi)$ is given by

$$\begin{aligned} \lambda(\phi) &= (\cot^2(\theta) + k_y^2 + 1)^{-1} (e \cos(\phi \sin(\theta)) + 1)^{-4} \\ &\times (e + 1)^2 (k_y \cos(\phi)) (e \cos(\phi \sin(\theta)) + 1) \\ &+ \sin(\phi) ((e + 1) \cos(\phi \sin(\theta)) + e k_y \sin(\theta) \sin(\phi \sin(\theta))))^2 \\ &+ (e + 1)^2 (k_y \sin(\phi)) (e \cos(\phi \sin(\theta)) + 1) \\ &- \cos(\phi) ((e + 1) \cos(\phi \sin(\theta)) + e k_y \sin(\theta) \sin(\phi \sin(\theta))))^2 \\ &+ (e + 1)^2 \cos^2(\theta) ((e + 1) \csc(\theta) \cos(\phi \sin(\theta)) \\ &+ e k_y \sin(\phi \sin(\theta)))^2. \end{aligned} \quad (53)$$

When $k_y = 0, k_z = \cot(\theta)$, we have

$$dl = d\phi = 0, \quad (54)$$

$$\lambda(\phi) = \frac{(e + 1)^4 \cos^2(\phi \sin(\theta))}{(e \cos(\phi \sin(\theta)) + 1)^4}, \quad (55)$$

which means two orbits are confined to the same cone and when $R_1 = R$, two orbits have intersection, $\lambda = 0$. By analyzing Eq. (52), we conclude that only when $k_y = 0$, $k_z = \cot(\theta)$, $\phi = \frac{(\frac{1}{2} + l)\pi}{\sin \theta}$, where l is integer, we have $\lambda = 0$. For other cases, $\lambda > 0$. By using Eqs. (33) and (52), we plot $\lambda(\phi(t))$ as function of t by choosing $\theta = \pi/2 \times 0.3, e = 0.5$ in Fig. 7. Dashed lines represent the case $dl = 0$ while solid lines represent the case $dl \neq 0$.

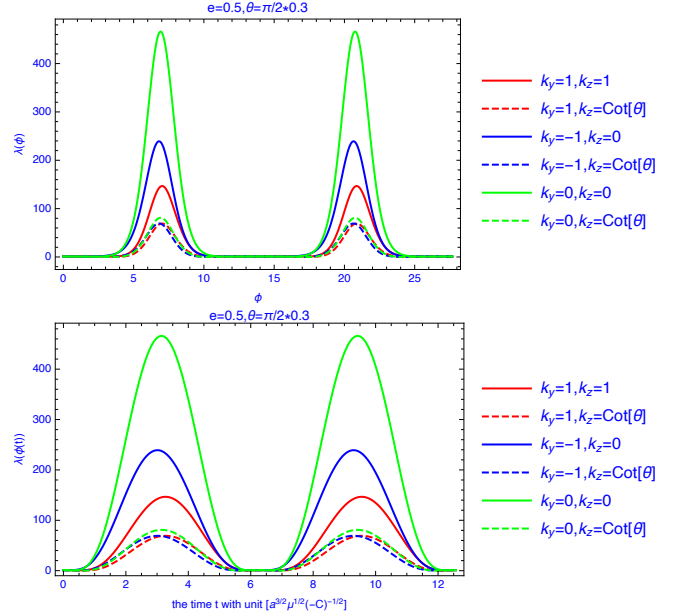


FIG. 7. [Upper panel] The plot of $\lambda(\phi)$ as a function of ϕ by choosing $\theta = \pi/2 \times 0.3$ and $e = 0.5$, according to (52). [Bottom panel] The plot of $\lambda(\phi(t))$ as a function of t by choosing $\theta = \pi/2 \times 0.3$ and $e = 0.5$. Dashed lines represent the case $dl = 0$ while solid lines represent the case $dl \neq 0$. For each period, there are exponential growths (decreases) in time, which imply the Lyapunov exponents.

For the case, $dx = 0$ and $dy \neq 0$, we can set

$$\mathbf{R}_1(0) - \mathbf{R}(0) = (dx, dy, dz) = (0, 1, k_z) \frac{dr}{\sqrt{1 + k_z^2}}. \quad (56)$$

By using Eq. (42), λ can be expressed as

$$\begin{aligned} \lambda(\phi) &= (k_z^2 + 1)^{-1} (e \cos(\phi \sin(\theta)) + 1)^{-4} \\ &\times ((e + 1)^2 (e \sin(\theta) \sin(\phi) \sin(\phi \sin(\theta))) \\ &+ e \cos(\phi) \cos(\phi \sin(\theta)) + \cos(\phi))^2 \\ &+ (e + 1)^2 (e \sin(\phi) \cos(\phi \sin(\theta)) \\ &- e \sin(\theta) \cos(\phi) \sin(\phi \sin(\theta))) \\ &+ \sin(\phi)^2 + (e(e + 1) \cos(\theta) \sin(\phi \sin(\theta)) \\ &+ k_z (e \cos(\phi \sin(\theta)) + 1)^2)^2. \end{aligned} \quad (57)$$

For the case, $dx = 0$, $dy = 0$, $dz \neq 0$, we have

$$da = de = 0, \quad dl = -dz, \quad (58)$$

$$\mathbf{R}_1(\phi) - \mathbf{R}(\phi) = (0, 0, dz), \quad (59)$$

which means $\lambda(\phi) = 1$ is a constant.

We have observed, as expected for the conserved autonomous systems, that the relative ratio of two neighboring orbits during their evolutions is periodic as a function of ϕ and also as a function of time. For each period, there are exponential growths (decreases) in time, which imply the Lyapunov exponents. The Lyapunov exponents are not essential for the next sections, so are not computed. Physically, this means that nearby orbits exponentially separate and approach from each other.

Particularly when $|D| \ll L$, we have

$$\cos \theta = |D|/L = \left(1 + \frac{|C|}{D^2} \mu a (1 - e^2)\right)^{-1/2}, \quad (60)$$

$$\sin \theta \simeq 1, \quad (61)$$

and the orbit is given by

$$\mathbf{R} \simeq \frac{a(1 - e^2)}{1 + e \cos(\phi)} \begin{pmatrix} \cos \phi \\ \sin \phi \\ \left(1 + \frac{|C|}{D^2} \mu a (1 - e^2)\right)^{-1/2} \end{pmatrix}. \quad (62)$$

In the limiting case of $D = 0$, the orbit becomes the Keplerian on the equatorial plane ($\theta = \pi/2$).

Now that we have a description for the effective one-body motion, we will calculate the emissions of energy and angular momentum for the $e = 0$ case in the next section

IV. ELECTROMAGNETIC RADIATION AND GRAVITATIONAL RADIATION

In this section, we only consider the case of $e = 0$, i.e the circular orbits and leave the case of $e \neq 0$ for future work. By using the quasi-static approximation², we will calculate the total emission rate of energy and angular momentum due to gravitational radiation and electromagnetic radiation.

A. Electromagnetic radiation

We first calculate the emission of electromagnetic radiation from electric charges on the orbit (35), averaged

over an orbital period. Then we consider the emission from magnetic charges in the same orbit and finally superimpose their fields. This derivation follows the same procedure as [35, 41].

Following [35, 41], the vector potential A at \mathbf{r} ($r \gg a$) is given by

$$A^i \simeq \frac{P^{ij}}{\sqrt{4\pi r}} \dot{Q}^j, \quad (63)$$

where

$$Q^i = q_1 x_1^i + q_2 x_2^i = \mu \Delta \sigma_q R^i, \quad (64)$$

is the electric charge dipole, $P^{ij} = \delta^{ij} - n^i n^j$ is the transverse projection, and

$$\Delta \sigma_q = q_2/m_2 - q_1/m_1. \quad (65)$$

The energy emission due to electric charges is given by

$$P_e = \frac{2\mu^2 (\Delta \sigma_q)^2}{3} \ddot{R}^i \ddot{R}_i. \quad (66)$$

The average energy loss over an orbital period T due to electric charges is given by

$$\begin{aligned} \bar{P}_e &= \frac{1}{T_1} \int_0^{2\pi} d\phi P_e \dot{\phi}^{-1} \\ &= \frac{2C^2 (\Delta \sigma_q)^2 \csc^2(\theta)}{3a^4} \end{aligned} \quad (67)$$

The angular momentum emission due to electric charges is given by

$$j_e^i = -\epsilon_{ijk} \frac{2}{3} \dot{Q}^j \ddot{Q}^k = -\frac{2\mu^2 (\Delta \sigma_q)^2}{3} \epsilon_{ijk} \dot{R}^j \ddot{R}^k, \quad (68)$$

For the angular momentum loss due to electromagnetic radiation averaged one orbital period T , we have

$$\left\langle \frac{dJ_e^i}{dt} \right\rangle \equiv \frac{1}{T_1} \int_0^{T_1} dt j_e^i. \quad (69)$$

For $e = 0$, we can get

$$j_e^1 = j_e^2 = \langle j_e^1 \rangle = \langle j_e^2 \rangle = 0, \quad (70)$$

$$\langle j_e^3 \rangle = j_e^3 = -\frac{2(-C)^{3/2} \sqrt{\mu} (\Delta \sigma_q)^2 \csc(\theta)}{3a^{5/2}}. \quad (71)$$

A great consequence of the enhanced symmetry due to the existence of magnetic monopoles is that Maxwell's equations and thus the classical dynamics of all the fields and charges remain invariant under the dual transformation

$$\begin{aligned} \mathbf{E}' &= \mathbf{E} \cos \alpha - \mathbf{B} \sin \alpha, \\ \mathbf{B}' &= \mathbf{E} \sin \alpha + \mathbf{B} \cos \alpha, \\ q' &= q \cos \alpha + g \sin \alpha, \\ g' &= g \cos \alpha - q \sin \alpha. \end{aligned} \quad (72)$$

² The quasi-static approximation is that the emission is approximated constant for the duration of one averaging period.

If we pick the transformation parameter $\alpha = \pi/2$, we can go from a situation containing only electric charges, to one containing only magnetic charges. This will allow us to immediately find the fields emanating from magnetic charges on the orbit from our results in this subsection. We can then superimpose them to find the total emission. For $\alpha = \pi/2$, we see

$$\begin{aligned} \mathbf{E}_2 &= - \left(\frac{\Delta\sigma_g}{\Delta\sigma_e} \right) \mathbf{B}_1, \\ \mathbf{B}_2 &= + \left(\frac{\Delta\sigma_g}{\Delta\sigma_e} \right) \mathbf{E}_1, \end{aligned} \quad (73)$$

where $\Delta\sigma_g$ determines the magnetic charge dipole:

$$\Delta\sigma_g = g_2/m_2 - g_1/m_1. \quad (74)$$

Here, we have used the connection between the electric and magnetic fields and the vector potential (63) to infer their proportionality with the charges.

In fact, we need not superimpose the fields - we may instead superimpose their emissions. This is not something we can do in general since the superposition principle of the Maxwell theory applies only to the fields, but we show in the following that it applies for this specific situation of adding together dual fields. A way to immediately, conceptually show that this is correct, is to notice that, far away on a shell where we calculate the emissions, the electric and magnetic fields from the electric charges are perpendicular to those from the magnetic charges, while the electric (magnetic) fields from the electric charges are parallel with the magnetic (electric) fields from the magnetic charges, and so, in superimposing the fields, the cross-terms vanish.

We explicitly show this by considering the integrated energy- and angular momentum density on a shell for electric and magnetic fields, naming the fields from the electric charge configuration $\mathbf{E}_1, \mathbf{B}_1$, and those from the dual transform $\mathbf{E}_2, \mathbf{B}_2$. Notice that the electric charge dipole has the same direction as the magnetic charge dipole does. So, we have $\mathbf{E}_1 \perp \mathbf{E}_2, \mathbf{B}_1 \perp \mathbf{B}_2, \mathbf{E}_1 \parallel \mathbf{B}_2, \mathbf{E}_2 \parallel \mathbf{B}_1$. Now we look at the result for the energy density and momentum density:

$$\begin{aligned} u &= \frac{1}{2} (E^2 + B^2) = \frac{1}{2} (E_1^2 + B_1^2 \\ &+ E_2^2 + B_2^2 + 2(\mathbf{E}_1 \cdot \mathbf{E}_2 + \mathbf{B}_1 \cdot \mathbf{B}_2)) = u_1 + u_2 \end{aligned} \quad (75)$$

$$\begin{aligned} \mathcal{P} &= \mathbf{E} \times \mathbf{B} = \mathbf{E}_1 \times \mathbf{B}_1 + \mathbf{E}_2 \times \mathbf{B}_2 \\ &+ \mathbf{E}_1 \times \mathbf{B}_2 + \mathbf{E}_2 \times \mathbf{B}_1 = \mathcal{P}_1 + \mathcal{P}_2. \end{aligned} \quad (76)$$

Note that

$$P = -r^2 \int d\Omega \hat{r} \cdot \mathcal{P}, \quad (77)$$

$$\mathbf{j} = -r^2 \int d\Omega \mathbf{r} \times \mathcal{P}, \quad (78)$$

we have

$$\bar{P}_{EM} = \left(1 + \left(\frac{\Delta\sigma_g}{\Delta\sigma_e} \right)^2 \right) \bar{P}_1, \quad (79)$$

$$\bar{\mathbf{j}}_{EM} = \left(1 + \left(\frac{\Delta\sigma_g}{\Delta\sigma_e} \right)^2 \right) \bar{\mathbf{j}}_1. \quad (80)$$

This means that our final results for the energy- and angular momentum emissions from our binary system are

$$\bar{P}_{EM} = \frac{2C^2((\Delta\sigma_q)^2 + (\Delta\sigma_g)^2) \csc^2(\theta)}{3a^4}, \quad (81)$$

$$\langle \bar{\mathbf{j}}_{EM} \rangle = - \frac{2(-C)^{3/2} \sqrt{\mu} ((\Delta\sigma_q)^2 + (\Delta\sigma_g)^2) \csc(\theta)}{3a^{5/2}} \quad (82)$$

Following [35], the gravitational field or electromagnetic field carries away a total angular momentum J , which is made of an orbital angular momentum contribution and of a spin contribution. This total angular momentum is drained from the total angular momentum of the source, which, for our binary system or any macroscopic source, is a purely and totally orbital angular momentum. So, the loss rates of the energy and angular momentum in our binary system due to electromagnetic radiation are given by

$$\left\langle \frac{dE_{EM}}{dt} \right\rangle = - \frac{2C^2((\Delta\sigma_q)^2 + (\Delta\sigma_g)^2) \csc^2(\theta)}{3a^4}, \quad (83)$$

$$\left\langle \frac{dL_{EM}}{dt} \right\rangle = - \frac{2(-C)^{3/2} \sqrt{\mu} ((\Delta\sigma_q)^2 + (\Delta\sigma_g)^2) \csc(\theta)}{3a^{5/2}}, \quad (84)$$

from which we find

$$\frac{\langle \frac{dL_{EM}}{dt} \rangle}{\langle \frac{dE_{EM}}{dt} \rangle} = \sqrt{(-C)\mu} a^3 \sin(\theta) = (-C)\mu a^2/L. \quad (85)$$

B. Gravitational radiation

Now, we compute the total radiated power in GWs. In our reference frame where \mathbf{L} is along z axis, the second mass moment can be written as

$$M^{ij} = \mu R^i R^j. \quad (86)$$

Following [42], the radiated power of GWs is expressed as

$$P_{GW} = \frac{1}{5} \left\langle \ddot{M}_{ij} \ddot{M}_{ij} - \frac{1}{3} \left(\ddot{M}_{kk} \right)^2 \right\rangle \quad (87)$$

Using Eqs. (36) and (86), one has

$$\begin{aligned}
\ddot{M}_{11} &= \frac{4(-C)^{3/2} \csc(\theta) \sin(2\phi)}{a^{5/2} \sqrt{\mu}}, \\
\ddot{M}_{12} &= -\frac{4(-C)^{3/2} \csc(\theta) \cos(2\phi)}{a^{5/2} \sqrt{\mu}}, \\
\ddot{M}_{13} &= \frac{(-C)^{3/2} \cot(\theta) \csc(\theta) \sin(\phi)}{a^{5/2} \sqrt{\mu}}, \\
\ddot{M}_{22} &= -\frac{8(-C)^{3/2} \csc(\theta) \sin(\phi) \cos(\phi)}{a^{5/2} \sqrt{\mu}}, \\
\ddot{M}_{23} &= -\frac{(-C)^{3/2} \cot(\theta) \csc(\theta) \cos(\phi)}{a^{5/2} \sqrt{\mu}}, \\
\ddot{M}_{33} &= 0.
\end{aligned} \tag{88}$$

Therefore, we obtain

$$P_{GW} = -\frac{(-C)^3 (15 \cos(2\theta) - 17) \csc^4(\theta)}{5a^5 \mu}, \tag{89}$$

which is independent of ϕ . The energy of GWs is only well-defined by taking an average over several periods. In our case, a well-defined quantity is the average of P_{GW} over one period T_1 . Thus we perform this time average to get the total radiated power

$$\bar{P}_{GW} \equiv \frac{1}{T_1} \int_0^{T_1} dt P_{GW} = P_{GW}, \tag{90}$$

and the average energy loss over an orbital period T_1 , which is given by

$$\left\langle \frac{dE_{GW}}{dt} \right\rangle = -\bar{P}_{GW} = \frac{(-C)^3 (15 \cos(2\theta) - 17) \csc^4(\theta)}{5a^5 \mu}. \tag{91}$$

Following [43], the rate of angular momentum emission due to GWs is given by

$$\frac{dL_{GW}^i}{dt} = -\frac{2}{5} \epsilon^{ikl} \langle \ddot{M}_{ka} \ddot{M}_{la} \rangle \tag{92}$$

For the angular momentum loss due to gravitational radiation averaged one orbital period T_1 , we have

$$\left\langle \frac{dL_{GW}^i}{dt} \right\rangle \equiv \frac{1}{T_1} \int_0^{T_1} dt \dot{L}_{GW}^i. \tag{93}$$

For the case of $e = 0$, i.e circular orbits, we get

$$\dot{L}_{GW}^1 = \frac{12(-C)^{5/2} \cot(\theta) \csc(\theta) \cos(\phi)}{5a^{7/2} \sqrt{\mu}}, \tag{94}$$

$$\dot{L}_{GW}^2 = \frac{12(-C)^{5/2} \cot(\theta) \csc(\theta) \sin(\phi)}{5a^{7/2} \sqrt{\mu}}, \tag{95}$$

from which follows

$$\left\langle \dot{L}_{GW}^1 \right\rangle = \left\langle \dot{L}_{GW}^2 \right\rangle = 0, \tag{96}$$

while we have the nonvanishing average

$$\left\langle \dot{L}_{GW}^3 \right\rangle = \dot{L}_{GW}^3 = \frac{(-C)^{5/2} (15 \cos(2\theta) - 17) \csc^3(\theta)}{5a^{7/2} \sqrt{\mu}}. \tag{97}$$

Because \mathbf{L} is along z axis, we may conclude that the loss rates of the energy and angular momentum in our binary system due to gravitational radiation are

$$\left\langle \frac{dE_{GW}}{dt} \right\rangle = \frac{(-C)^3 (15 \cos(2\theta) - 17) \csc^4(\theta)}{5a^5 \mu}, \tag{98}$$

$$\left\langle \frac{dL_{GW}}{dt} \right\rangle = \frac{(-C)^{5/2} (15 \cos(2\theta) - 17) \csc^3(\theta)}{5a^{7/2} \sqrt{\mu}}, \tag{99}$$

and we may show the ratio

$$\frac{\left\langle \frac{dL_{GW}}{dt} \right\rangle}{\left\langle \frac{dE_{GW}}{dt} \right\rangle} = \sqrt{(-C)\mu} a^3 \sin(\theta) = (-C)\mu a^2 / L. \tag{100}$$

From the results for the electromagnetic and gravitational radiations, we can show that for any θ and a

$$\frac{\left\langle \frac{dE_{GW}}{dt} \right\rangle}{\left\langle \frac{dE_{EM}}{dt} \right\rangle} = \frac{\left\langle \frac{dL_{GW}}{dt} \right\rangle}{\left\langle \frac{dL_{EM}}{dt} \right\rangle}. \tag{101}$$

C. Evolutions of a and θ

For the static orbit, θ and a are constants. However, when the emissions of energy and angular momentum due to the gravitational and electromagnetic radiations are included, θ and a become functions of time t . In this subsection, we will explore the evolutions of a and θ .

The total emission rates of energy and angular momentum due to gravitational and electromagnetic radiations are given, respectively, by

$$\left\langle \frac{dE}{dt} \right\rangle = \left\langle \frac{dE_{EM}}{dt} \right\rangle + \left\langle \frac{dE_{GW}}{dt} \right\rangle, \tag{102}$$

$$\left\langle \frac{dL}{dt} \right\rangle = \left\langle \frac{dL_{EM}}{dt} \right\rangle + \left\langle \frac{dL_{GW}}{dt} \right\rangle. \tag{103}$$

According to

$$E = \frac{C}{2a}, \tag{104}$$

$$L = \frac{\sqrt{-\mu C a}}{\sin(\theta)}, \tag{105}$$

we have the rates of the semimajor axis and the conic angle

$$\begin{aligned}
\frac{da}{dt} &= \frac{4C((\Delta\sigma_q)^2 + (\Delta\sigma_g)^2) \csc^2(\theta)}{3a^2} \\
&+ \frac{2C^2(15 \cos(2\theta) - 17) \csc^4(\theta)}{5a^3 \mu}, \tag{106}
\end{aligned}$$

$$\frac{d\theta}{dt} = \frac{2C(\Delta\sigma_q)^2 + (\Delta\sigma_g)^2 \cot(\theta)}{3a^3} + \frac{C^2(15 \cos(2\theta) - 17) \cot(\theta) \csc^2(\theta)}{5a^4\mu}. \quad (107)$$

Noting that the first part and the second part separately have the same form $da/d\theta$, as will be shown below, and using the chain rule for differentiation, we may find

$$\frac{da}{d\theta} = 2a \csc(\theta) \sec(\theta), \quad (108)$$

$$a = c_0 \tan^2(\theta), \quad (109)$$

where c_0 is determined by the initial condition $a = a_0$ when $\theta = \theta_0$. From Eq. (105) and

$$\cos(\theta) = |D|/L, \quad (110)$$

we have

$$c_0 = \frac{D^2}{-\mu C}. \quad (111)$$

Now we get the evolution of the orbit and then calculate the merger time of the dyonic binary. For any θ and a , Eq. (101) is explicitly given by

$$\frac{\langle \frac{dE_{GW}}{dt} \rangle}{\langle \frac{dE_{EM}}{dt} \rangle} = \frac{\langle \frac{dL_{GW}}{dt} \rangle}{\langle \frac{dL_{EM}}{dt} \rangle} = \frac{3C(15 \cos(2\theta) - 17) \csc^2(\theta)}{10a((\Delta\sigma_q)^2 + (\Delta\sigma_g)^2)\mu}. \quad (112)$$

The binary system spends most of the decay time in a state for which $a \approx a_0$. For a given a_0 , the total rate of energy and angular momentum emission is dominated by gravitational radiation or electromagnetic radiation which depends on m_1, m_2, q_1, q_2, g_1 and g_2 .

First, we consider the case where electromagnetic radiation dominates gravitational radiation at $a \approx a_0$. When $D = 0$ or $\theta = \pi/2$, we have

$$\frac{da}{dt} = \frac{4C((\Delta\sigma_q)^2 + (\Delta\sigma_g)^2)}{3a^2}, \quad (113)$$

$$\frac{d\theta}{dt} = 0, \quad (114)$$

which gives the coalescence time

$$\tau_{EM}(a_0, \theta = \frac{\pi}{2}) = \int_{a_0}^0 da \left(\frac{da}{dt}\right)^{-1} = \frac{-a_0^3}{4C((\Delta\sigma_q)^2 + (\Delta\sigma_g)^2)}. \quad (115)$$

On the other hand, when $D \neq 0$ or $\theta \neq \pi/2$, Eqs. (106) and (107) become

$$\frac{da}{dt} = \frac{4C((\Delta\sigma_q)^2 + (\Delta\sigma_g)^2) \csc^2(\theta)}{3a^2}, \quad (116)$$

$$\frac{d\theta}{dt} = \frac{2C((\Delta\sigma_q)^2 + (\Delta\sigma_g)^2) \cot(\theta)}{3a^3}. \quad (117)$$

So, we have

$$\frac{da}{d\theta} = 2a \csc(\theta) \sec(\theta) \quad (118)$$

$$a = c_0 \tan^2(\theta). \quad (119)$$

Then we found

$$\left(\frac{d\theta}{dt}\right)^{-1} = \frac{3c_0^3 \tan^7(\theta)}{2C((\Delta\sigma_q)^2 + (\Delta\sigma_g)^2)}. \quad (120)$$

For the orbit, we can integrate Eq. (116) requiring $a(t) = 0$ at $t = \tau_{EM}(a_0, \theta_0)$ or, equivalently, we can integrate Eq. (117) requiring $\theta(t) = 0$ at $t = \tau_{EM}(a_0, \theta_0)$, since we have seen that at the coalescence θ goes to zero. Since the analytic expression for $a(\theta)$ is simpler than the form of the inverse function $\theta(a)$, it is much better to use Eq. (118) and get

$$\int_0^{\tau_{EM}(a_0, \theta_0)} dt = \int_{\theta_0}^0 d\theta \left(\frac{d\theta}{dt}\right)^{-1}, \quad (121)$$

$$\tau_{EM}(a_0, \theta_0) = -\frac{a_0^3 F_1(\theta_0)}{4C((\Delta\sigma_q)^2 + (\Delta\sigma_g)^2)}, \quad (122)$$

where

$$F_1(\theta_0) = \frac{1}{2 \tan^6(\theta_0)} (2 \sec^6(\theta_0) - 9 \sec^4(\theta_0) + 18 \sec^2(\theta_0) + 12 \log(\cos(\theta_0)) - 11), \quad (123)$$

$$\tan(\theta_0) = \frac{\sqrt{-\mu C a_0}}{|D|}. \quad (124)$$

We plot $F_1(\theta_0)$ as a function of θ_0 in Fig. 8. When $\theta_0 \rightarrow 0$, $F_1(\theta_0) \rightarrow 0$ while $\theta_0 \rightarrow \pi/2$, $F_1(\theta_0) \rightarrow 1$, which is consistent with Eq. (115) and [35].

Next, we consider the case where gravitational radiation dominates electromagnetic radiation at $a \approx a_0$. When $D = 0$ or $\theta = \pi/2$, we obtain

$$\frac{da}{dt} = \frac{-64C^2}{5a^3\mu}, \quad (125)$$

$$\frac{d\theta}{dt} = 0, \quad (126)$$

which gives the merger time

$$\tau_{GM}(a_0, \theta = \frac{\pi}{2}) = \int_{a_0}^0 da \left(\frac{da}{dt}\right)^{-1} = \frac{5a_0^4\mu}{256C^2}. \quad (127)$$

In the other case where $D \neq 0$ or $\theta \neq \pi/2$, Eqs. (106) and (107) become

$$\frac{da}{dt} = \frac{2C^2(15 \cos(2\theta) - 17) \csc^4(\theta)}{5a^3\mu}, \quad (128)$$

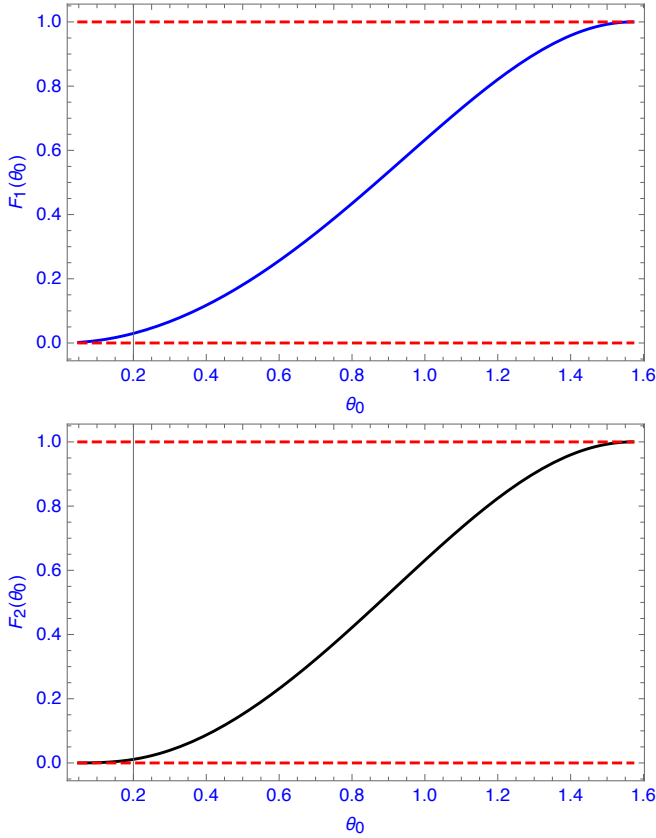


FIG. 8. Upper: The plot of $F_1(\theta_0)$ as a function of θ_0 . Bottom: The plot of $F_2(\theta_0)$ as a function of θ_0

$$\frac{d\theta}{dt} = \frac{C^2(15 \cos(2\theta) - 17) \cot(\theta) \csc^2(\theta)}{5a^4\mu}. \quad (129)$$

The functional dependence of $da/d\theta$ has the same form as Eq. (118). Similarly, the coalescence time for the gravitational-radiation dominated merger is given by

$$\tau_{GW}(a_0, \theta_0) = \frac{5a_0^4\mu F_2(\theta_0)}{256C^2}, \quad (130)$$

where

$$\begin{aligned} F_2(\theta_0) = & \frac{1}{245760 \tan^8(\theta_0)} (245760 \sec^8(\theta_0) \\ & - 1331200 \sec^6(\theta_0) + 3043200 \sec^4(\theta_0) \\ & - 4124400 \sec^2(\theta_0) - \log(15 \sin^2(\theta_0) + 1) \\ & - 2097150 \log(\cos(\theta_0)) + 2166640). \end{aligned} \quad (131)$$

We plot $g_2(\theta_0)$ as a function of θ_0 in Fig. 8. When $\theta_0 \rightarrow 0$, $F_2(\theta_0) \rightarrow 0$ while $\theta_0 \rightarrow \pi/2$, $F_2(\theta_0) \rightarrow 1$, which is consistent with Eq. (115) and [35]. From Eqs. (123) and (131), when θ_0 goes near zero, $F_1(\theta_0)$ and $F_2(\theta_0)$ can be much smaller than unit (e.g. $F_1(\pi/20) = 0.018$, $F_2(\pi/20) = 0.005$), which implies the electric and magnetic charges or θ_0 could significantly suppress the merger time of the dyonic binary. As θ_0 approaches zero, the binary coalesces immediately and τ_{EM} and τ_{GW} vanish, as expected. But this case corresponds to the general relativistic regime, which requires methods beyond the post-Newtonian method.

V. CONCLUSION

Dyonic black holes have attracted much attention not only in theoretical study but also in recent observations of GWs. In this paper, we have derived the effective one-body motion of the dyonic binary and explore features of the static orbit including the chaotic behavior. By using the post-Newtonian method, we have calculated the total emission rate of energy and angular momentum due to the gravitational radiation and electromagnetic radiation for circular orbits on a Poincaré Cone. Moreover, we have found the evolution of a , θ and calculated the merger time of the dyonic binary. It has been shown that the electric and magnetic charges can significantly suppress the merger time of the dyonic binary no matter what the gravitational radiation or the electromagnetic radiation dominates. The results of this paper provide rich information on the dyonic binary and may be used to test black holes with magnetic charges.

ACKNOWLEDGMENTS

This work is supported in part by the National Natural Science Foundation of China Grants No.11690021, No.11690022, No.11851302, No.11821505, and No.11947302, in part by the Strategic Priority Research Program of the Chinese Academy of Sciences Grant No. XDB23030100, No. XDA15020701 and by Key Research Program of Frontier Sciences, CAS. The work of S.P.K. was supported in part by National Research Foundation of Korea (NRF) funded by the Ministry of Education (2019R1I1A3A01063183).

[1] B. P. Abbott *et al.* (LIGO Scientific, Virgo), *Phys. Rev. Lett.* **116**, 061102 (2016), arXiv:1602.03837 [gr-qc].
 [2] B. P. Abbott *et al.* (LIGO Scientific, Virgo), *Phys. Rev. Lett.* **116**, 241103 (2016), arXiv:1606.04855 [gr-qc].
 [3] B. P. Abbott *et al.* (LIGO Scientific, Virgo), *Phys. Rev.* **X6**, 041015 (2016), [erratum: *Phys. Rev.* X8,no.3,039903(2018)], arXiv:1606.04856 [gr-qc].

[4] B. P. Abbott *et al.* (LIGO Scientific, VIRGO), *Phys. Rev. Lett.* **118**, 221101 (2017), [Erratum: *Phys. Rev. Lett.* 121,no.12,129901(2018)], arXiv:1706.01812 [gr-qc].
 [5] B. P. Abbott *et al.* (LIGO Scientific, Virgo), *Astrophys. J.* **851**, L35 (2017), arXiv:1711.05578 [astro-ph.HE].
 [6] B. P. Abbott *et al.* (LIGO Scientific, Virgo), *Phys. Rev. Lett.* **119**, 141101 (2017), arXiv:1709.09660 [gr-qc].

- [7] B. P. Abbott *et al.* (LIGO Scientific, Virgo), *Phys. Rev. X* **9**, 031040 (2019), arXiv:1811.12907 [astro-ph.HE].
- [8] S. Bird, I. Cholis, J. B. Muoz, Y. Ali-Hamoud, M. Kamionkowski, E. D. Kovetz, A. Raccanelli, and A. G. Riess, *Phys. Rev. Lett.* **116**, 201301 (2016), arXiv:1603.00464 [astro-ph.CO].
- [9] M. Sasaki, T. Suyama, T. Tanaka, and S. Yokoyama, *Phys. Rev. Lett.* **117**, 061101 (2016), [erratum: *Phys. Rev. Lett.* 121,no.5,059901(2018)], arXiv:1603.08338 [astro-ph.CO].
- [10] S. Clesse and J. Garca-Bellido, *Phys. Dark Univ.* **15**, 142 (2017), arXiv:1603.05234 [astro-ph.CO].
- [11] Y. Ali-Hamoud, E. D. Kovetz, and M. Kamionkowski, *Phys. Rev. D* **96**, 123523 (2017), arXiv:1709.06576 [astro-ph.CO].
- [12] K. Belczynski, D. E. Holz, T. Bulik, and R. O’Shaughnessy, *Nature* **534**, 512 (2016), arXiv:1602.04531 [astro-ph.HE].
- [13] J. Casares and P. G. Jonker, *Space Sci. Rev.* **183**, 223 (2014), arXiv:1311.5118 [astro-ph.HE].
- [14] J. M. Corral-Santana, J. Casares, T. Muoz-Darias, P. Rodriguez-Gil, T. Shahbaz, M. A. P. Torres, C. Zurita, and A. A. Tyndall, *Science* **339**, 1048 (2013), arXiv:1303.0034 [astro-ph.GA].
- [15] J. M. Corral-Santana, J. Casares, T. Munoz-Darias, F. E. Bauer, I. G. Martinez-Pais, and D. M. Russell, *Astron. Astrophys.* **587**, A61 (2016), arXiv:1510.08869 [astro-ph.HE].
- [16] Z.-C. Chen and Q.-G. Huang, *Astrophys. J.* **864**, 61 (2018), arXiv:1801.10327 [astro-ph.CO].
- [17] M. Raidal, C. Spethmann, V. Vaskonen, and H. Veerme, *JCAP* **1902**, 018 (2019), arXiv:1812.01930 [astro-ph.CO].
- [18] L. Liu, Z.-K. Guo, and R.-G. Cai, *Phys. Rev. D* **99**, 063523 (2019), arXiv:1812.05376 [astro-ph.CO].
- [19] L. Liu, Z.-K. Guo, and R.-G. Cai, *Eur. Phys. J. C* **79**, 717 (2019), arXiv:1901.07672 [astro-ph.CO].
- [20] S. Hawking, *Mon. Not. Roy. Astron. Soc.* **152**, 75 (1971).
- [21] B. J. Carr and S. W. Hawking, *Mon. Not. Roy. Astron. Soc.* **168**, 399 (1974).
- [22] R. Bean and J. Magueijo, *Phys. Rev. D* **66**, 063505 (2002), arXiv:astro-ph/0204486 [astro-ph].
- [23] M. Kawasaki, A. Kusenko, and T. T. Yanagida, *Phys. Lett. B* **711**, 1 (2012), arXiv:1202.3848 [astro-ph.CO].
- [24] B. Carr and J. Silk, *Mon. Not. Roy. Astron. Soc.* **478**, 3756 (2018), arXiv:1801.00672 [astro-ph.CO].
- [25] J. Schwinger, *Physical Review* **144**, 1087 (1966).
- [26] M. Kasuya, *Phys. Rev. D* **25**, 995 (1982).
- [27] K. A. Bronnikov, *Phys. Rev. D* **63**, 044005 (2001), arXiv:gr-qc/0006014.
- [28] Y. Shnir, *Magnetic monopoles* (2005).
- [29] M. Staelens (MoEDAL), in *Meeting of the Division of Particles and Fields of the American Physical Society* (2019) arXiv:1910.05772 [hep-ex].
- [30] N. E. Mavromatos and V. A. Mitsou, arXiv e-prints, arXiv:2005.05100 (2020), arXiv:2005.05100 [hep-ph].
- [31] A. D. Linde, *Phys. Lett. B* **327**, 208 (1994), arXiv:astro-ph/9402031.
- [32] K.-M. Lee, V. Nair, and E. J. Weinberg, *Phys. Rev. D* **45**, 2751 (1992), arXiv:hep-th/9112008.
- [33] M. S. Volkov and D. V. Gal’tsov, *Phys. Rept.* **319**, 1 (1999), arXiv:hep-th/9810070.
- [34] J. Maldacena, (2020), arXiv:2004.06084 [hep-th].
- [35] L. Liu, Z.-K. Guo, R.-G. Cai, and S. P. Kim, (2020), arXiv:2001.02984 [astro-ph.CO].
- [36] C.-M. Chen, S. P. Kim, J.-R. Sun, and F.-Y. Tang, *Phys. Rev. D* **95**, 044043 (2017), arXiv:1607.02610 [hep-th].
- [37] P. G. L. Leach and G. P. Flessas, arXiv e-prints, math-ph/0403028 (2004), arXiv:math-ph/0403028 [math-ph].
- [38] J. Schwinger, K. A. Milton, W.-Y. Tsai, J. Deraad, Lester L., and D. C. Clark, *Annals of Physics* **101**, 451 (1976).
- [39] D. Zwanziger, *Physical Review* **176**, 1480 (1968).
- [40] J. H. Argyris, G. Faust, M. Haase, and R. Friedrich, *An exploration of dynamical systems and chaos; 2nd ed.* (Springer, Berlin, 2015).
- [41] . Christiansen, J. B. Jimnez, and D. F. Mota, (2020), arXiv:2003.11452 [gr-qc].
- [42] P. C. Peters and J. Mathews, *Phys. Rev.* **131**, 435 (1963).
- [43] P. C. Peters, *Phys. Rev.* **136**, B1224 (1964).